

Observation of a Plastic Crystal in Water–Ammonia Mixtures under High Pressure and Temperature

H. Zhang, F. Datchi, L. Andriambarijaona, M. Rescigno, L. E. Bove, S. Klotz, and S. Ninet*



Cite This: *J. Phys. Chem. Lett.* 2023, 14, 2301–2307



Read Online

ACCESS |



Metrics & More

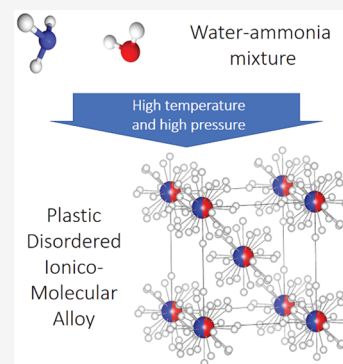


Article Recommendations



Supporting Information

ABSTRACT: Solid mixtures of ammonia and water, the so-called ammonia hydrates, are thought to be major components of solar and extra-solar icy planets. We present here a thorough characterization of the recently reported high pressure (P)–temperature (T) phase VII of ammonia monohydrate (AMH) using Raman spectroscopy, X-ray diffraction, and quasi-elastic neutron scattering (QENS) experiments in the ranges 4–10 GPa, 450–600 K. Our results show that AMH-VII exhibits common structural features with the disordered ionic-molecular alloy (DIMA) phase, stable above 7.5 GPa at 300 K: both present a substitutional disorder of water and ammonia over the sites of a body-centered cubic lattice and are partially ionic. The two phases however markedly differ in their hydrogen dynamics, and QENS measurements show that AMH-VII is characterized by free molecular rotations around the lattice positions which are quenched in the DIMA phase. AMH-VII is thus a peculiar crystalline solid in that it combines three types of disorder: substitutional, compositional, and rotational.



The physics of water, ammonia, and other molecules under extreme P – T conditions has been a topic of intense research in the last decades, for its importance in many fields and in particular in the modeling of the interior of icy planets and their satellites.^{1,2} One remarkable finding is that for pressures above a few GPa and T below 300 K, the configurations of the oxygen and nitrogen sublattices—body-centered cubic (bcc) for water ice and quasi-hexagonal close-packed (hcp) for solid ammonia—are kept intact at least up to the Mbar (100 GPa) range.^{3–6} By contrast, pressure has a strong effect on the average position and dynamics of H atoms, driving the symmetrization of H bonds in H_2O ^{7–10} and ionization of NH_3 ^{11–13} at low T . Coupling high temperatures to high pressures gives rise to other dynamic regimes for the hydrogen atoms where plastic states, characterized by free rotations of the molecules around their lattice positions,^{14–19} and superionic states, characterized by fast diffusion of the protons through the oxygen or nitrogen lattice,^{19–25} can be promoted. In contrast with the pure ices, there is still little known on the properties and phase diagram of their mixtures under extreme P – T conditions despite the fact that they are more relevant systems for planetary modeling. At ambient pressure, the ammonia–water mixtures crystallize in three stoichiometric compounds, known as ammonia hydrates, with, respectively, 1:2, 1:1, and 2:1 ammonia to water ratios. We focus here on the 1:1 compound, ammonia monohydrate (AMH). Early neutron studies have mapped the phase diagram of AMH up to 7 GPa and below 300 K, finding several molecular phases termed I to VI.^{26,27} AMH-VI, formed above 6.5 GPa and 270 K, is of particular interest as it was described as a disordered molecular alloy (DMA) where water and

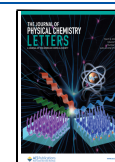
ammonia randomly occupy the sites of a simple bcc structure. More recently, Liu et al.²⁸ found that the DMA phase is actually a partially ionic phase, where ammonia and water coexist with NH_4^+ and OH^- ions, in about a 2:1 molecular to ionic ratio at 10 GPa and 300 K. DMA was thus renamed DIMA for the disordered ionic-molecular alloy. Liu et al.²⁸ also found that the DIMA phase may coexist with a purely ionic and ordered phase of $P4/nmm$ space group, predicted as the ground state by calculations²⁹ but only seen in minor proportion in experiments. AMH-VI is thus a variable mixture of the DIMA and $P4/nmm$ phases, and the question whether one is more stable than the other has not been settled yet.

At high T , Zhang et al.³⁰ recently reported that another AMH phase, named AMH-VII, becomes stable above 3.6 GPa–324 K and up to at least 8.3 GPa–675 K. AMH-VII melts congruently, showing that it has the same 1:1 stoichiometry as the liquid, but no other structural information has been made available to date. Interestingly, computer simulations based on the density functional theory (DFT)^{29,31–33} have predicted the existence of plastic and superionic states in ammonia hydrates appearing at P – T conditions compatible with the range of stability of AMH-VII. Directly probing these exotic states by experiment is very challenging as this requires techniques sensitive to H atom

Received: January 11, 2023

Accepted: February 16, 2023

Published: February 27, 2023



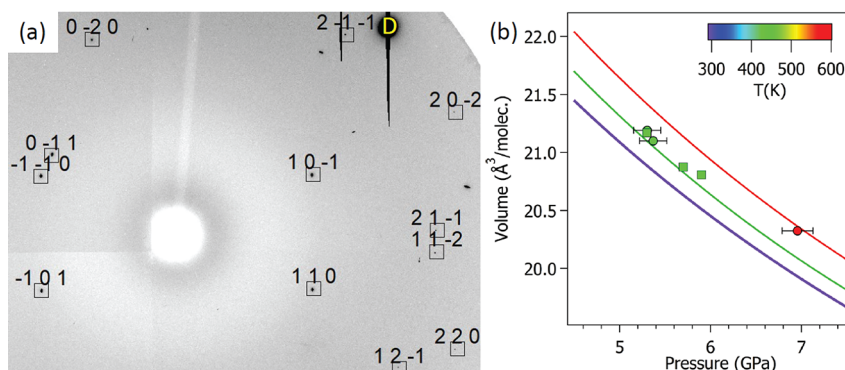


Figure 1. (a) Details of the diffraction image of a single crystal AMH-VII at 5.4 GPa and 453 K overlaid with the indexing of reflections. The saturated spots noted D are from the diamond anvils. (b) Molecular volume vs pressure in AMH. The symbols represent the measured volumes of AMH-VII at high temperature. The purple curve is a fit to experimental data at 300 K (see SI Section S2.2). The green and red lines are the calculated EOS at 450 and 550 K, respectively, using the thermal dilatation coefficient of ice VII³⁶ as an estimate for that of AMH.

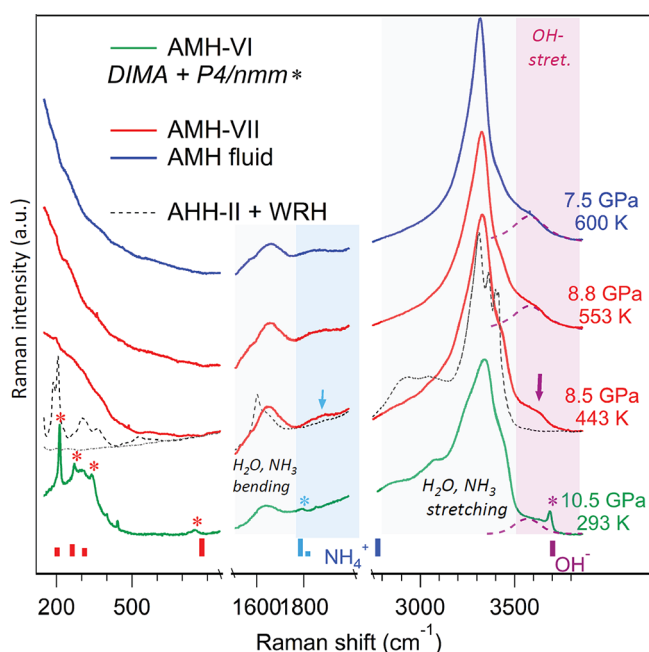


Figure 2. Comparison between the measured Raman spectra of AMH-VI (green), AMH-VII (red), AMH-fluid (blue), and AHH-II + WRH (gray dotted line) at P - T conditions indicated in the figure. The frequency windows 1200–1400 cm^{-1} and 2300–2700 cm^{-1} dominated by, respectively, the first- and second-order Raman signals from the diamond anvils have been omitted. The bottom ticks and asterisks represent the peak positions for the $P4/nmm$ phase predicted by DFT and experimentally observed,²⁸ respectively. The arrows emphasize bands assigned to ionic species in AMH-VII.

mobility, such as neutron scattering, proton NMR, and conductivity measurements, which are difficult to combine with extreme P - T conditions.

In this letter, we report on the structural and dynamic properties of AMH-VII determined by a combination of X-ray diffraction (XRD), Raman scattering, and quasi-elastic neutron scattering experiments (QENS). Recent advances in QENS techniques^{34,35} enabled us to measure the self-dynamics structure factor of AMH to the record pressure of 8.6 GPa. Our results demonstrate that AMH-VII is a crystalline plastic form of the DIMA phase where molecular (H_2O , NH_3) and ionic species (OH^- and NH_4^+) are randomly arranged on a

body-centered cubic (bcc) lattice and present a dynamic rotational disorder of the hydrogen atoms.

Experimental methods are presented in detail in the Supporting Information (SM). *In situ* HP measurements were made in diamond anvil cells (DAC) for XRD and Raman scattering and in the Paris–Edinburg press (PE) for neutron scattering. Synchrotron XRD experiments were performed at the PSICHE beamline of SOLEIL (Saint Aubin, France) and the ID27 beamline of ESRF (Grenoble, France), and QENS experiments were performed at the IN6-Sharp beamline of ILL (Grenoble, France).

In order to determine the structure of AMH-VII, we grew single crystals by slowly compressing the liquid at temperatures above 324 K until a single crystal germ crystallized and filled the sample chamber. Part of a diffraction image collected at 5.4 GPa and 453 K is shown in Figure 1a. All observed reflections could be indexed by a unique bcc unit cell with $a = 3.4809(1)$ \AA . A single structural solution was found by ShelXT³⁷ in space group $Im\bar{3}m$, which contains one atomic site for oxygen and nitrogen atoms at $(0, 0, 0)$, replicated by symmetry at $(0.5, 0.5, 0.5)$. This implies substitutional disorder for O and N. Using an equal O/N occupation as imposed by stoichiometry, the refinement with ShelXL³⁸ converged to an R1-factor of 4.7% (see SI Table 1). We note however that the refinement is not sensitive to the O/N occupation, due to the small difference in the number of electrons ($\Delta Z = 1$) and likely to the absence of H atoms in the structural model. As a matter of fact, we could not locate any H atoms from the difference Fourier map, which suggests that they are all disordered. As far as the position of the O/N atoms is concerned, the structure of AMH-VII is thus identical to that reported for the DMA²⁶ or DIMA²⁸ phases at room temperature.

For all studied AMH-VII samples—either single crystals formed as above or polycrystals obtained by heating powder samples (Figure S1 in the SI for a diffraction pattern of a polycrystalline sample), no evidence of the $P4/nmm$ phase observed to coexist with DIMA at 300 K²⁸ was found. The measured molecular volumes in the intervals 5–7 GPa and 433–570 K are shown in Figure 1b. When taking thermal expansion into account, they agree very well with the equation of state of AMH-DIMA at 300 K (see SI Section S2.2 and Figure S2), confirming that AMH-VII is a single phase with the same 1:1 stoichiometry as the loaded mixture.

As recalled above, the unique difference between the structural models of DMA and DIMA is that the former is a

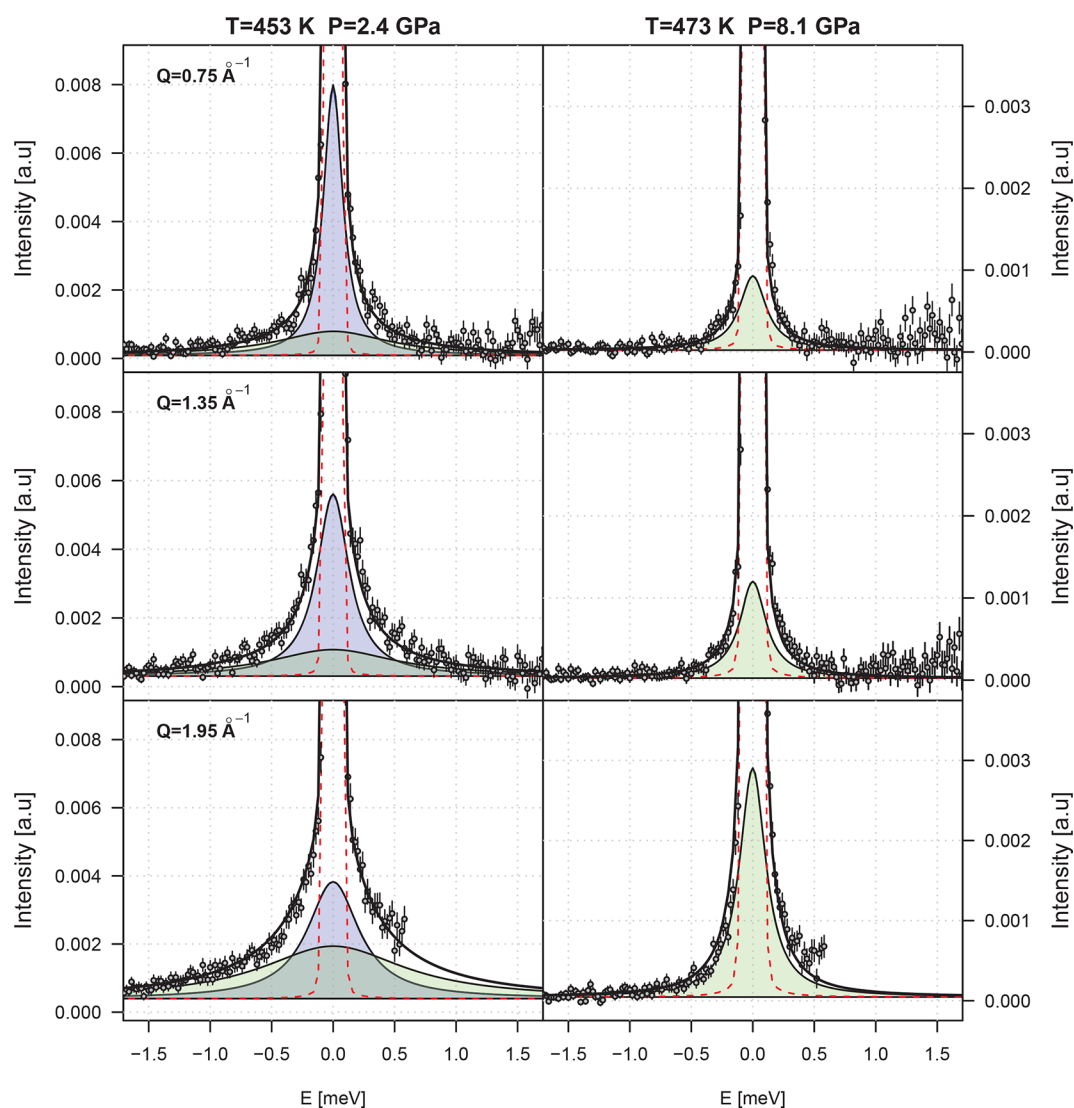


Figure 3. Examples of QENS spectra obtained in the liquid (left) at 2.4(6) GPa–450 K and AMH-VII (right) phases at 8.1(3) GPa–473 K for selected values of Q . Black symbols with error bars are experimental data; the red dotted line is the instrumental resolution, and the blue and green lines represent the translational and rotational components obtained from fits, respectively.

purely molecular alloy while the latter also contains OH^- and NH_4^+ ions. The question thus arises whether AMH-VII is purely molecular (DMA-like) or a mixed molecular-ionic (DIMA-like) alloy. To answer this, we measured the Raman spectrum of AMH-VII at various P – T . The Raman spectrum of AMH-VII at 8.5 GPa–443 K and 8.8 GPa–553 K are compared in Figure 2 to those of AMH-VI (DIMA+ $P4/nmm$) at 10 GPa–293 K, the equimolar liquid at 7.5 GPa–600 K, and the demixed sample AHH-II+WRH³⁰ at 8.7 GPa–415 K.

Comparison of the Raman spectra of phases VII and VI reveals both strong similarities and singularities. First, the Raman peaks assigned to the molecular species NH_3 and H_2O (the O–H and N–H stretching modes at 3000–3500 cm^{-1} and the bending modes around 1600 cm^{-1}) are located in the same frequency ranges in phases VII and VI and have similar shapes. Their broad bandwidths are typical of hydrogen disordered phases (see SI Figure S3 for a tentative deconvolution of the stretching band). Second, the sharp peak centered at 3700 cm^{-1} in AMH-VI is absent in AMH-VII. The former was assigned to the OH^- stretching mode in the ionic $P4/nmm$ phase at 300 K²⁸ (see Figure 2); thus, its

absence in the AMH-VII samples is consistent with our XRD observations above. On the contrary, the broad band centered at 3600 cm^{-1} (pink peak in Figure 2) is present in both AMH-VI and AMH-VII but not in the molecular phases. Calculations in ref 28 showed that this band most likely corresponds to OH^- stretching modes in the DIMA phase, which is also consistent with the fact that it hardens with pressure as in $P4/nmm$ (see SI Figure S4). Its broader bandwidth in the DIMA (RT) and AMH-VII (HT) phases compared to $P4/nmm$ can be explained by the substitutional disorder in the former two, leading to various possible environments for the ions, and/or by a shorter lifetime of these ions.

Finding the spectroscopic signature of NH_4^+ ions is more difficult as their N–H stretching frequencies are expected around 2800–2900 cm^{-1} , which is close to the strong second-order Raman band of the diamond anvils. The NH_4^+ twisting modes, by contrast, are well isolated (around 1850 cm^{-1} in $P4/nmm$), and we observe a weak and broad band in this region for AMH-VII but not for the molecular phases. Here again the broad bandwidth is assigned to disorder.

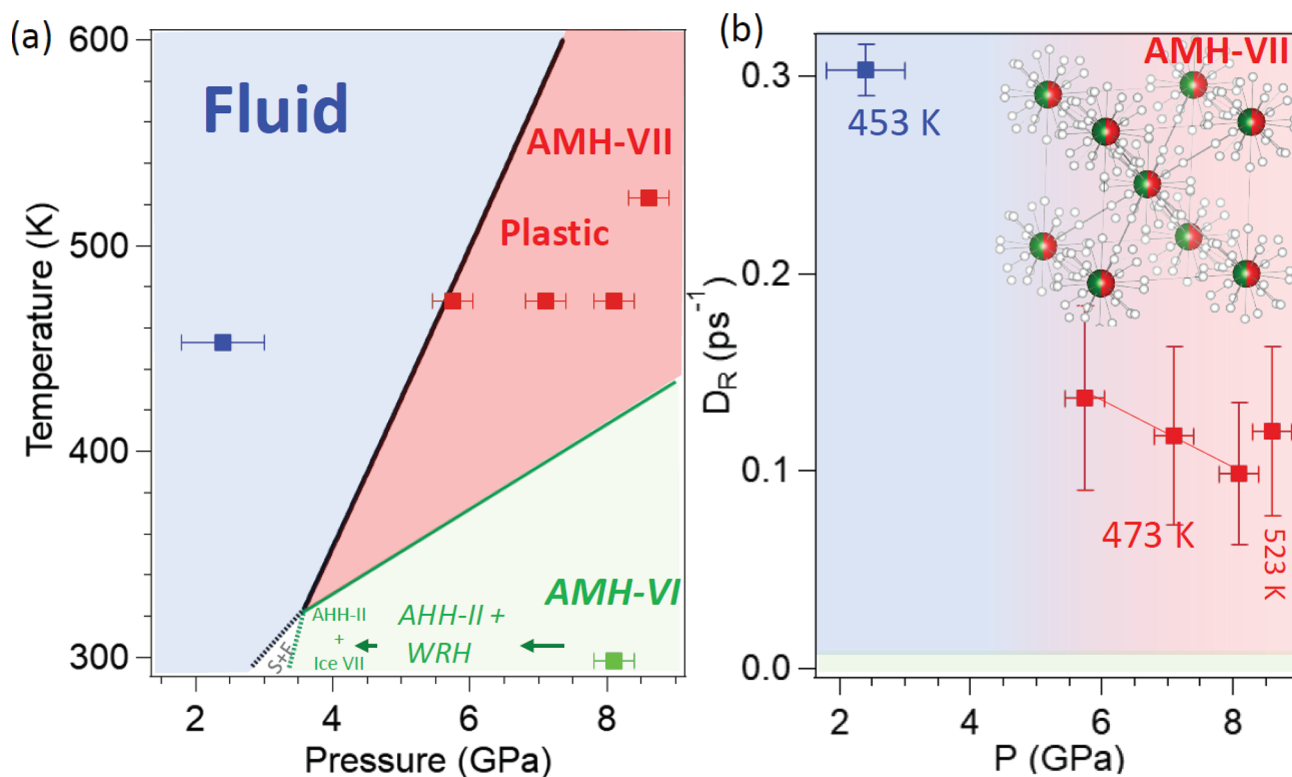


Figure 4. (a) Phase diagram of AMH. The symbols show P – T points where QENS data were collected. (b) Evolution of the rotational diffusion coefficient as a function of pressure for different temperatures. The inset shows a schematic description of the unit cell of the plastic AMH-VII.

Moving to the low-frequency range, a marked difference can be observed: AMH-VII presents a strong, featureless Raman activity extending from 500 cm^{-1} down to the lowest measurable frequency (90 cm^{-1}), while the Raman spectrum of AMH-VI contains three sharp peaks assigned to the lattice modes of $P4/nmm$,²⁸ riding over a broad band [100 – 400 cm^{-1}] from the DIMA phase. The intensity difference (AMH-VII – AMH-VI) in the lattice region, shown in SI Figure S5, is evidence of an additional Raman activity in AMH-VII at frequencies below 200 cm^{-1} whose intensity increases with temperature. Such a low-frequency signal, together with the broadening or disappearance of the lattice modes, has been identified as signatures of a plastic crystal in NH_3 -II,³⁹ β - N_2 ,⁴⁰ and other molecular systems.^{41,42} It can also be seen in Figure 2 that the Raman spectrum of AMH-VII is very similar to that of the liquid phase at 7.5 GPa, a feature which has been previously noted in pure ammonia between the liquid and the plastic phases II and III.⁴³

To obtain direct evidence of plasticity, we performed QENS measurements on an equimolar mixture of D_2O and NH_3 in the range 2–8.6 GPa, 300–523 K. Owing to the very large incoherent scattering cross section of H atoms compared to that of oxygen, nitrogen, or deuterium, the incoherent quasi-elastic scattered signal from a hydrogenated sample is dominated by the scattering processes from the H atoms in the molecules. QENS experiments are thus well suited for studying the single-particle dynamics of hydrogenated molecules, which includes both the molecular scale translational diffusion and rotational relaxation. The use of deuterated water was chosen here both to reduce the amount of multiple scattering and autoabsorption of the sample and to focus on the ammonia molecule reorientational dynamics.

A selection of QENS spectra as a function of exchanged energy E and wavevector Q are shown in Figure 3 for the liquid and AMH-VII (see SI Figure S6 for additional data), and the investigated P – T points are indicated in the phase diagram of Figure 4a. At high T and low Q , the vibrational, translational, and reorientational motions of the molecules are decoupled⁴⁴ and the QENS spectra can be modeled by a sum of Lorentzian functions whose width is proportional to the time scales of molecular diffusion and rotation. The details of the data reduction, fit function, and procedure are given in SI Section S4. The best fit curves and their components are reported in Figure 3 (see also SI Figure S6).

In the liquid phase, both a translational and a rotational contribution are observed. The measured molecular translational $D_T = 1.1(2) \times 10^5\text{ cm}^2/\text{s}$ and reorientational $D_R = 0.30(5)\text{ ps}^{-1}$ diffusion coefficients are, respectively, about 1/6 and 1/2 the ones measured in liquid water at similar P – T conditions.⁴⁵ To our knowledge, there is no corresponding data in the literature for ammonia at these P – T conditions.

For all P – T points corresponding to the AMH-VII solid, we observed that the translational diffusion is frozen but the rotational dynamics is still active, although the rotations slow down by about a factor of 3 [see the evolution of D_R with pressure in Figure 4b]. By contrast, no broadening of the elastic peak other than the instrumental resolution is observed at 8.1 GPa–300 K, showing that the molecules do not rotate in the ambient temperature phase VI (see SI Figure S7). We may thus conclude that AMH-VII is a plastic solid to at least 8.6 GPa and 523 K, although further experiments are needed in order to probe the H motions in water molecules. We note in this regard that pure water ice has been predicted^{14,15,46} to become a plastic bcc ice in a similar P – T range above 352 K–6 GPa,¹⁵ so it is likely that water molecules also rotate in bcc

AMH-VII. As seen in Figure 4b, D_R is, within uncertainties, independent of pressure and temperature conditions in the plastic solid VII. This behavior can be understood taking into account that, in the limited P range investigated here, the hydrogen bond strength has a very weak variation due to the low compressibility of the crystal. Moreover, the number of first neighbors of molecules remains constant, both with pressure and with temperature, and the molecular rotation is not phonon assisted. By contrast, in the liquid, the molecular rotation is coupled and assisted by the molecular translational diffusion; therefore, the reorientational motion is faster and has a stronger dependence on the thermodynamic conditions.^{45,47,48}

In summary, the present work shows that AMH-VII is built on the same *bcc* structure with substitutional O/N disorder as the room-temperature DIMA and is also composed of ions and molecules with molecular species in major proportions. Conversely, the rotational dynamics in AMH-VII markedly differs from that of DIMA, and we show through QENS experiments that the present species freely rotate as in a plastic solid. AMH-VII is thus a crystalline plastic form of the room-temperature DIMA phase, compiling three types of disorder: substitutional, compositional (molecules and ions), and rotational. Plasticity has been recently predicted in AMH by *ab initio* molecular dynamics simulations,³² starting from the H-ordered and fully ionic *P4/nmm* phase. It would be interesting to determine how the initial substitutional and compositional disorder of DIMA influences the onset of plasticity; however, such calculations are challenging as they require large simulation boxes to account for disorder. We found no evidence in the present QENS experiments for proton diffusive motion in AMH-VII up to 8 GPa and 523 K, as one would expect in the superionic state. This indicates that superionicity requires higher P – T conditions where both rotational and translational protonic motions are active, as observed in pure water ice.²² Reference 32 reported the onset of superionic conduction in AHH around 10 GPa and 600 K, that is, slightly higher P – T conditions than achieved in the present experiments, and probably within reach of the QENS technique in the near future. Finally, the P – T domain of stability of plastic AMH-VII is close to the present conditions in some Jovian satellites such as Titan, Ariel, and Enceladus^{49,50} and sub-Neptune size exoplanets.⁵¹ Its presence during the formation of these bodies should thus be taken into consideration.

■ ASSOCIATED CONTENT

SI Supporting Information

The Supporting Information is available free of charge at <https://pubs.acs.org/doi/10.1021/acs.jpcllett.3c00092>.

Additional experimental methods are available: details of X-ray diffraction experiments (including structure of AMH-VII, equation of state of AMH), Raman experiments (including Raman spectra of AMH-VII and VI, pressure evolution) and quasi-elastic neutron scattering experiments (including methods, data analysis, QENS spectra of AMH-VII and liquid and their comparison with AMH-VII, and Q dependence of the HWHM of the rotational term and QISF of AMH-VII (PDF)

Transparent Peer Review report available (PDF)

■ AUTHOR INFORMATION

Corresponding Author

S. Ninet – Institut de Minéralogie, de Physique des Matériaux et de Cosmochimie (IMPMC), Sorbonne Université, CNRS UMR 7590, MNHN, Paris 75005, France; orcid.org/0000-0001-8239-4725; Email: sandra.ninet@sorbonne-universite.fr

Authors

H. Zhang – Institut de Minéralogie, de Physique des Matériaux et de Cosmochimie (IMPMC), Sorbonne Université, CNRS UMR 7590, MNHN, Paris 75005, France; Shandong Key Laboratory of Optical Communication Science and Technology, School of Physics Science and Information Technology, Liaocheng University, Liaocheng 252059, China

F. Datchi – Institut de Minéralogie, de Physique des Matériaux et de Cosmochimie (IMPMC), Sorbonne Université, CNRS UMR 7590, MNHN, Paris 75005, France; orcid.org/0000-0003-1252-1770

L. Andriambarijaona – Institut de Minéralogie, de Physique des Matériaux et de Cosmochimie (IMPMC), Sorbonne Université, CNRS UMR 7590, MNHN, Paris 75005, France

M. Rescigno – Dipartimento di Fisica, Università di Roma La Sapienza, 00185 Roma, Italy

L. E. Bove – Institut de Minéralogie, de Physique des Matériaux et de Cosmochimie (IMPMC), Sorbonne Université, CNRS UMR 7590, MNHN, Paris 75005, France; Dipartimento di Fisica, Università di Roma La Sapienza, 00185 Roma, Italy; LQM, Institute of Physics, Ecole Polytechnique Fédérale de Lausanne, CH-1015 Lausanne, Switzerland; orcid.org/0000-0003-1386-8207

S. Klotz – Institut de Minéralogie, de Physique des Matériaux et de Cosmochimie (IMPMC), Sorbonne Université, CNRS UMR 7590, MNHN, Paris 75005, France

Complete contact information is available at:

<https://pubs.acs.org/10.1021/acs.jpcllett.3c00092>

Notes

The authors declare no competing financial interest.

■ ACKNOWLEDGMENTS

We acknowledge K. Béneut for the use of the spectroscopy platform at IMPMC; B. Baptiste and L. Delbes for the use of the XRD platform at IMPMC and B. Baptiste for his advices in the structure refinement. We acknowledge also the SOLEIL and ESRF synchrotrons and the Institut Laue-Langevin (ILL) for the provision of beam time to proposals 20170522 and 20180575 (SOLEIL), HS2185 (ESRF), and 7-03-153 (ILL - <https://dx.doi.org/10.5291/ILL-DATA.7-03-153>); and J.P. Itié (SOLEIL), N. Guignot (SOLEIL), M. Mezouar (ESRF), G. Garbarino (ESRF), and M. Koza (ILL) for their assistance in the experiments. We acknowledge financial support from the french Agence Nationale de la Recherche under Grants No. ANR-15-CE30-0008-01 (SUPER-ICES) and No. ANR-13-IS04-0006-01 (PACS). This work was also supported by the Chinese Scholarship Council through the allocation of a scholarship to Haiwa Zhang and the French state funds managed by the ANR within the Investissements d'Avenir program under Grant No. ANR-11-IDEX-0004-02, and more specifically within the framework of the Cluster of Excellence MATISSE led by Sorbonne Université.

REFERENCES

- (1) Guillot, T. Interiors of Giant Planets Inside and Outside the Solar System. *Science* **1999**, *286*, 72–77.
- (2) Sohl, F.; Solomonidou, A.; Wagner, F. W.; Coustenis, A.; Hussmann, H.; Schulze-Makuch, D. Structural and tidal models of Titan and inferences on cryovolcanism. *Journal of Geophysical Research: Planets* **2014**, *119*, 1013–1036.
- (3) Kuhs, W. F.; Finney, J. L.; Vettier, C.; Bliss, D. V. Structure and hydrogen ordering in ices VI, VII, and VIII by neutron powder diffraction. *J. Chem. Phys.* **1984**, *81*, 3612–3623.
- (4) Wolanin, E.; Pruzan, P.; Chervin, J. C.; Canny, B.; Gauthier, M.; Häusermann, D.; Hanfland, M. Equation of state of ice VII up to 107 GPa. *Phys. Rev. B* **1997**, *56*, 5781.
- (5) Ninet, S.; Datchi, F.; Klotz, S.; Hamel, G.; Loveday, J. S.; Nelmes, R. J. Hydrogen bonding in ND₃ probed by neutron diffraction to 24 GPa. *Phys. Rev. B* **2009**, *79*, No. 100101(R).
- (6) Datchi, F.; Ninet, S.; Gauthier, M.; Saitta, A. M.; Canny, B.; Decremps, F. Solid ammonia at high pressure: A single-crystal x-ray diffraction study to 123 GPa. *Phys. Rev. B* **2006**, *73*, 174111.
- (7) Holzapfel, W. On the Symmetry of the Hydrogen Bonds in Ice VII. *J. Chem. Phys.* **1972**, *56*, 712–715.
- (8) Benoit, M.; Marx, D.; Parrinello, M. Tunnelling and zero-point motion in high-pressure ice. *Nature* **1998**, *392*, 258.
- (9) Aoki, K.; Yamawaki, H.; Sakashita, M.; Fujihisa, H. Infrared absorption study of the hydrogen-bond symmetrization in ice to 110 GPa. *Phys. Rev. B* **1996**, *54*, 15673.
- (10) Goncharov, A. F.; Struzhkin, V. V.; Somayazulu, M. S.; Hemley, R. J.; Mao, H.-K. Raman Spectroscopy of Dense H₂O and The Transition to Symmetric Hydrogen Bonds. *Science* **1996**, *273*, 218.
- (11) Pickard, C.; Needs, R. Highly compressed ammonia forms an ionic crystal. *Nat. Mater.* **2008**, *7*, 775.
- (12) Ninet, S.; Datchi, F.; Dumas, P.; Mezouar, M.; Garbarino, G.; Mafey, A.; Pickard, C. J.; Needs, R. J.; Saitta, A. M. Experimental and theoretical evidence for an ionic crystal of ammonia at high pressure. *Phys. Rev. B* **2014**, *89*, 174103.
- (13) Palasyuk, T.; Troyan, I.; Eremets, M.; Drozd, V.; Medvedev, S.; Zaleski-Ejgierd, P.; Magos-Palasyuk, E.; Wang, H.; Bonev, S. A.; Dudenko, D.; Naumov, P. Ammonia as a case study for the spontaneous ionization of a simple hydrogen-bonded compound. *Nat. Commun.* **2014**, *5*, 3460.
- (14) Takii, Y.; Koga, K.; Tanaka, H. A plastic phase of water from computer simulation. *J. Chem. Phys.* **2008**, *128*, 204501.
- (15) Aragones, J. L.; Vega, C. Plastic crystal phases of simple water models. *J. Chem. Phys.* **2009**, *130*, 244504.
- (16) Hirata, M.; Yagasaki, T.; Matsumoto, M.; Tanaka, H. Phase Diagram of TIP4P/2005 Water at High Pressure. *Langmuir* **2017**, *33*, 11561–11569.
- (17) Doverspike, M. A.; Liu, S. B.; Ennis, P.; Johnson, T.; Conradi, M. S.; Luszczyński, K.; Norberg, R. E. NMR in high pressure phases of solid NH₃ and ND₃. *Phys. Rev. B* **1986**, *33*, 14.
- (18) Ninet, S.; Datchi, F. High pressure-high temperature phase diagram of ammonia. *J. Chem. Phys.* **2008**, *128*, 154508.
- (19) Ninet, S.; Datchi, F.; Saitta, A. M. Proton Disorder and Superionicity in Hot Dense Ammonia Ice. *Phys. Rev. Lett.* **2012**, *108*, 165702.
- (20) Cavazzoni, C.; Chiarotti, G. L.; Scandolo, S.; Tosatti, E.; Bernasconi, M.; Parrinello, M. Superionic and metallic states of water and ammonia at giant planet conditions. *Science* **1999**, *283*, 44–46.
- (21) Goncharov, A. F.; Goldman, N.; Fried, L. E.; Crowhurst, J. C.; Kuo, I.-F. W.; Mundy, C. J.; Zaug, J. M. Dynamic Ionization of Water under Extreme Conditions. *Phys. Rev. Lett.* **2005**, *94*, 125508.
- (22) Queyroux, J.-A.; Hernandez, J.-A.; Weck, G.; Ninet, S.; Plisson, T.; Klotz, S.; Garbarino, G.; Guignot, N.; Mezouar, M.; Hanfland, M.; Itié, J.-P.; Datchi, F. Melting Curve and Isostructural Solid Transition in Superionic Ice. *Phys. Rev. Lett.* **2020**, *125*, 195501.
- (23) Weck, G.; Queyroux, J.-A.; Ninet, S.; Datchi, F.; Mezouar, M.; Loubeyre, P. Evidence and Stability Field of fcc Superionic Water Ice Using Static Compression. *Phys. Rev. Lett.* **2022**, *128*, 165701.
- (24) Millot, M.; Hamel, S.; Rygg, J. R.; Celliers, P. M.; Collins, G. W.; Coppari, F.; Fratanduono, D. E.; Jeanloz, R.; Swift, D. C.; Eggert, J. H. Experimental evidence for superionic water ice using shock compression. *Nat. Phys.* **2018**, *14*, 297–302.
- (25) Millot, M.; Coppari, F.; Rygg, J. R.; Correa Barrios, A.; Hamel, S.; Swift, D. C.; Eggert, J. H. Nanosecond X-Ray Diffraction of Shock-Compressed Superionic Water Ice. *Nature* **2019**, *569*, 251.
- (26) Loveday, J. S.; Nelmes, R. J. Ammonia Monohydrate VI: A Hydrogen-Bonded Molecular Alloy. *Phys. Rev. Lett.* **1999**, *83*, 4329.
- (27) Loveday, J. S.; Nelmes, R. J. The ammonia hydrates—model mixed hydrogen-bonded systems. *High Pressure Research* **2004**, *24*, 45.
- (28) Liu, C.; et al. Topologically Frustrated Ionisation in a Water-Ammonia Ice Mixture. *Nat. Commun.* **2017**, *8*, 1065.
- (29) Griffiths, G. I. G.; Misquitta, A. J.; Fortes, A. D.; Pickard, C. J.; Needs, R. J. High pressure ionic and molecular crystals of ammonia monohydrate within density functional theory. *J. Chem. Phys.* **2012**, *137*, 064506.
- (30) Zhang, H.; Datchi, F.; Andriambarijaona, L. M.; Zhang, G.; Queyroux, J. A.; Béneut, K.; Mezouar, M.; Ninet, S. Melting curve and phase diagram of ammonia monohydrate at high pressure and temperature. *J. Chem. Phys.* **2020**, *153*, 154503.
- (31) Bethkenhagen, M.; Cebulla, D.; Redmer, R.; Hamel, S. Superionic Phases of the 1:1 Water-Ammonia Mixture. *J. Phys. Chem. A* **2015**, *119*, 10582.
- (32) Naden Robinson, V.; Hermann, A. Plastic and superionic phases in ammonia–water mixtures at high pressures and temperatures. *J. Phys.: Condens. Matter* **2020**, *32*, 184004.
- (33) Jiang, X.; Wu, X.; Zheng, Z.; Huang, Y.; Zhao, J. Ionic and superionic phases in ammonia dihydrate NH₃·2H₂O under high pressure. *Phys. Rev. B* **2017**, *95*, 144104.
- (34) Klotz, S.; Strässle, T.; Bove, L. E. Quasi-elastic neutron scattering in the multi-GPa range and its application to liquid water. *Appl. Phys. Lett.* **2013**, *103*, 193504.
- (35) Komatsu, K.; Klotz, S.; Shinozaki, A.; Iizuka, R.; Bove, L. E.; Kagi, H. Performance of ceramic anvils for high pressure neutron scattering. *High Pressure Research* **2014**, *34*, 494–499.
- (36) Frank, M. R.; Fei, Y.; Hu, J. Constraining the equation of state of fluid H₂O to 80 GPa using the melting curve, bulk modulus, and thermal expansivity of Ice VII. *Geochim. Cosmochim. Acta* **2004**, *68*, 2781–2790.
- (37) Sheldrick, G. M. Integrated space-group and crystal-structure determination. *Acta Crystallographica Section A Foundations and Advances* **2015**, *71*, 3–8.
- (38) Sheldrick, G. *SHELX-97, Program for X-Ray Crystal Structure Solution*; Gottingen University: 1997.
- (39) Luo, R. K.; Nye, C.; Medina, F. D. Raman spectra of solid ammonia II. *J. Chem. Phys.* **1986**, *85*, 4903.
- (40) Medina, F. D.; Daniels, W. B. Raman spectrum of solid nitrogen at high pressures and low temperatures. *J. Chem. Phys.* **1976**, *64*, 150–161.
- (41) Hédoux, A.; Guinet, Y.; Capet, F.; Affouard, F.; Descamps, M. Raman effects under pressure in chloroadamantaneplastic crystal. *J. Phys.: Condens. Matter* **2002**, *14*, 8725–8741.
- (42) Salzillo, T.; Girlando, A.; Brillante, A. Revisiting the Disorder? Order Transition in 1?X-Adamantane Plastic Crystals: Rayleigh Wing, Boson Peak, and Lattice Phonons. *J. Phys. Chemistry C* **2021**, *125*, 7384–7391.
- (43) Kume, T.; Sasaki, S.; Shimizu, H. Raman Study of Solid Ammonia at High Pressure and Low Temperature. *J. Raman Spectrosc.* **2001**, *32*, 383.
- (44) Chen, S.-H.; Gallo, P.; Sciortino, F.; Tartaglia, P. Molecular-dynamics study of incoherent quasielastic neutron-scattering spectra of supercooled water. *Phys. Rev. E* **1997**, *56*, 4231–4243.
- (45) Bove, L. E.; Klotz, S.; Strässle, T.; Koza, M.; Teixeira, J.; Saitta, A. M. Translational and Rotational Diffusion in Water in the Gigapascal Range. *Phys. Rev. Lett.* **2013**, *111*, 185901.
- (46) Hernandez, J. A.; Caracas, R. Proton Dynamics and the Phase Diagram of Dense Water Ice. *J. Chem. Phys.* **2018**, *148*, 214501.

(47) Ranieri, U.; Giura, P.; Gorelli, F. A.; Santoro, M.; Klotz, S.; Gillet, P.; Paolasini, L.; Koza, M. M.; Bove, L. E. Dynamical Crossover in Hot Dense Water: The Hydrogen Bond Role. *J. Phys. Chem. B* **2016**, *120*, 9051–9059.

(48) Amann-Winkel, K.; Bellissent-Funel, M.-C.; Bove, L. E.; Loerting, T.; Nilsson, A.; Paciaroni, A.; Schlesinger, D.; Skinner, L. X-ray and Neutron Scattering of Water. *Chem. Rev.* **2016**, *116*, 7570–7589.

(49) Lunine, J. I.; Stevenson, D. J. Clathrate and ammonia hydrates at high pressure: Application to the origin of methane on Titan. *Icarus* **1987**, *70*, 61–77.

(50) Grasset, O.; Sotin, C.; Deschamps, F. On the internal structure and dynamics of Titan. *Planetary and Space Science* **2000**, *48*, 617–636.

(51) Léger, A.; Selsis, F.; Sotin, C.; Guillot, T.; Despois, D.; Mawet, D.; Ollivier, M.; Labèque, A.; Valette, C.; Brachet, F.; Chazelas, B.; Lammer, H. A new family of planets? Ocean-Planets. *Icarus* **2004**, *169*, 499–504.

Recommended by ACS

Multidirectional Polarization Impacts on Microwave Heating Efficiency: A Molecular Dynamics Research of Microwave Heating of Common Solvents

Hongxiao Shi, Dezhi Gou, *et al.*

JANUARY 18, 2023

THE JOURNAL OF PHYSICAL CHEMISTRY B

READ 

Molecular-Level Investigation of Hydrate–Anhydrous Phase Transformations of the Dapsone Structurally Related Compound 3,3'-Diaminophenyl Sulfone

Paola Paoli, Luca Conti, *et al.*

NOVEMBER 03, 2022

CRYSTAL GROWTH & DESIGN

READ 

Terahertz Spectroscopy and DFT Analysis of Phonon Dynamics of the Layered Van der Waals Semiconductor Nb₃X₈ (X = Cl, I)

Jangwon Kim, Jae Hoon Kim, *et al.*

APRIL 08, 2023

ACS OMEGA

READ 

Mechanical Properties of a New Hybrid Inorganic–Organic Framework: A Nanoindentation, High-Pressure X-ray Diffraction, and Computational Study

Li-Jun Ji, Wei Li, *et al.*

NOVEMBER 07, 2022

CRYSTAL GROWTH & DESIGN

READ 